Simultaneous Profiling of DNA Copy Number Variations and Transcriptional Programs in Single Cells using RNA-seq

Authors: Ali Madipour-Shirayeh[1], Natalie Erdmann[1], Chungyee Leung-Hagesteijn[1], Paola Neri[2], Ines Tagoug[1], Rodger E. Tiedemann[1,3*]

[1]Princess Margaret Cancer Centre, University Health Network, Toronto, Ontario, Canada

[2]Arnie Charbonneau Cancer Institute, University of Calgary, Alberta, Canada

[3]Departments of Medicine and Medical Biophysics, University of Toronto, Toronto, Ontario, Canada

*Senior and corresponding author: Rodger E. Tiedemann: rodger.tiedemann@uhn.ca

Key words:

single cell RNA sequencing (scRNA-seq), copy number variation (CNV), normalization, multi-omics, multiple myeloma, RTAM, sciCNV

SUMMARY

Chromosome copy number variations (CNVs) are a near-universal feature of cancer however their specific effects on cellular function are poorly understood. Single-cell RNA sequencing (scRNA-seq) can reveal cellular gene expression however cannot directly link this to CNVs. Here we report scRNA-seq normalization methods that improve gene expression alignment between cells, increasing the sensitivity of scRNA-seq for CNV detection. We also report sciCNV, a tool for inferring CNVs from scRNA-seq. Together, these tools enable dual profiling of DNA and RNA in single cells. We apply these techniques to multiple myeloma (MM) and examine the cellular effects of cancer CNVs +8q23-24 and +1q21-44. Primary MM cells with +8q23-24 upregulate MYC, MYC-target genes, mRNA processing and protein synthesis; but also upregulate DEPTOR and have smaller transcriptomes. MM cells with +1q21-44 instead reconfigure translation and suppress unfolded protein stress whilst increasing proliferation, oxidative phosphorylation and MCL1. Overall, we provide tools that can enhance the analysis of scRNA-seq and help reveal the effects of cancer CNVs on cellular reprogramming.

Genomic CNVs are a pervasive feature of cancer. Copy number gains on chromosome arms 8q, 1q, 3q and 5p are amongst the most common karyotype abnormalities in human cancer, yet the action of these and other CNVs on the molecular processes within cancer cells remains poorly understood[1,2].

ScRNA-seq can reveal the transcription state of single cells, however it cannot directly relate this to DNA lesions. Although physical sequencing of both DNA and RNA within single cells has been reported[3-5], and should enable pairing of CNVs with their transcriptional outcomes, existing techniques provide profiling of only a few cells and thus afford only a limited view of the genomic and transcriptional heterogeneity within any cancer. Furthermore, while CNVs and gene expression can be profiled in separate populations of cells and computationally integrated[6], this may not recapitulate the biological state of individual cells.

DNA CNVs can be inferred from scRNA-seq, which could thus be leveraged to provide both layers of omics information within individual cells. However, previously reported approaches[7-9] reveal constraints imposed by the sparsity of single-cell data. In particular, inconsistencies in the detection of lowly-expressed genes within single cells causes stochastic noise that influences transcriptome distribution and interferes with RNA-based CNV detection. Normalization is thus critical for accurate scRNA-seq interpretation[10-14] and for secondary CNV detection.

Here we report scRNA-seq normalization methods that reduce the influence of noise from lowly-expressed genes on single-cell transcriptome scale. These methods improve gene expression comparisons between cells and thus enhance the sensitivity of scRNA-seq for the detection of small expression changes arising from gene copy number differences. We also report sciCNV, a new tool for inferring CNVs in single cells from scRNA-seq. Together, these methods enable high-throughput profiling of both DNA copy number and RNA in the same cell, facilitating direct examination of the effects of cancer CNVs on gene expression programs at a cellular level.

RESULTS

Enhanced single-cell RNA-seq normalization methods: RTAM1 and -2

Single-cell RNA-seq enables gene expression comparisons between cells. However, the accuracy of such comparisons depends critically upon data normalization. As the best methods for normalizing scRNA-seq remain controversial, we developed RTAM1 and -2 (described in the **online methods** and **supplementary figures S1-3**) and compared the RTAM methods with other normalization strategies currently in use.

To compare the methods for their control of systemic and stochastic variations between cells due to size or sequence depth we generated scRNA-seq data for cells belonging uniformly to the B cell lineage (n>15,000) (**figure 1a**). We examined a single lineage in order to minimize confounding biological variation between cells due to their ancestry. However, we deliberately generated data from a mix of both small quiescent B cells and large transformed plasma cells to ensure that the normalization methods would be challenged by cells embodying a full spectrum of sizes and transcriptional activities. The cells were isolated from MM patient bone marrow samples by FACS and were profiled using the 10X Genomics single cell RNA-seq library kit. Cell- and gene-specific transcripts were enumerated using barcoded unique molecular identifiers (UMI).

The raw scRNA-seq data from one of three initial test samples is depicted in **figure 1b**. As shown, the distributions of transcript counts per gene varied significantly from cell to cell, reflecting differences in their cellular transcriptome sizes and demonstrating a clear need for normalization. The samples were next normalized using either TPM[15], SCRAN[11], SCONE[12] or Seurat's SCTransform function[16] (**figure 1b** and **supplementary figures S4-S20**). To compare the alignments of the normalized transcriptomes, we examined the mean and median expression in each cell of a curated list of housekeeping genes (HKG) known to be broadly expressed with low variation[9]. We also examined the average expression in each cell of all of the ubiquitously-expressed genes (UEG) detected in >95% of the cells in the sample. For each sample tested, the UEG represent the largest possible set of genes that are commonly expressed across the test cells. Whilst the expression of any individual gene is expected to vary between cells for both

biological and technical reasons, the average expression per cell of a large set of ubiquitous genes should be similar, particularly amongst cells of the same lineage, and its variance between cells provides a metric of normalization effectiveness.

As shown, TPM, which normalizes cellular transcriptomes primarily by their total transcript count, produced a very large variance in the average expression of HKG or UEG between cells, suggesting significant limitations for scRNA-seq application. By comparison, SCRAN and SCONE produced superior alignments of gene expression averages across cells. However, SCONE, which produced the better alignment, achieved this only by implementing quantile normalization – exchanging the actual distribution of transcript counts in each cell for a standardized distribution – which caused a loss of inter-cellular variation, particularly in highly-expressed genes. The expression of IGH or IGL genes, for example, a critical feature of plasma cells, was reduced by SCONE's quantile normalization into a virtual constant across cells (**supplementary figure S21**).

As each of these scRNA-seq normalization methods has limitations, we developed RTAM1 and -2. The RTAM approach originates from a consideration of the strengths and weaknesses of scRNA-seq. Whereas lowly expressed genes are detected within single cells with low resolution (due to low integer transcript counts) and show significant stochastic variation, highly expressed genes are robustly detected and show finer quantisation of variation relative to intensity. RTAM thus utilizes highly-expressed genes, whose expression is resolved with greater accuracy, to align cellular transcriptomes. Genes are ranked in each cell by their expression and the summed intensities of the top-ranked genes is standardized in log-space using unique non-linear cell- and gene-specific adjustments of gene expression determined either by cellular gene expression rank (RTAM1) or by gene expression intensity (RTAM2) (see **methods**).

Importantly, compared to TPM, SCTransform or SCRAN, both RTAM1 and RTAM2 reduce the cell-to-cell variance in the average (median or mean) expression of HKG and UEG sets (**figure 1c** and **supplementary figures S4-S20**). The coefficients of variation (CV) produced by each normalization method for the "average" expression of HKG or UEG in individual cells is shown in **figure 1d** and **supplemental figure S21a**, for 3 independent patient samples. As shown,

106 RTAM1 (red) and RTAM2 (blue) reduce variations in the average gene expression of single
107 cells, even when this average expression is calculated by 3 different methods. By design, the
108 RTAM methods also standardize the average expression of highly-expressed genes, and thus
109 overall these methods produce superior alignments of cellular transcriptomes and of gene
110 expression between cells. At the same time, both RTAM1 and RTAM2 maintain the original
111 variability observed between cells in the expression of individual highly-transcribed genes,
112 unlike the quantile normalization implemented by SCONE (**supplementary figure S21b-d**).
113 Overall, therefore, the RTAM methods represent useful new strategies for normalizing scRNA-
114 seq data that can enhance the accuracy of gene expression comparisons between cells.
115
116 **Single-cell inferred chromosomal copy number variation: sciCNV**
117 We next sought to develop a method for detecting single-cell chromosomal CNV from scRNA-
118 seq, leveraging the enhanced normalization provided by RTAM to increase the sensitivity of
119 single-cell transcriptomics for CNV detection. To optimize DNA copy number estimates from
120 gene expression, and to mitigate against data sparsity in single cells, we developed a two-
121 pronged approach, called sciCNV (described in the **supplemental methods**). Briefly, RTAM-
122 normalized gene expression data from single cells was aligned with matching data from pooled
123 control cells to develop expression disparity scores, which were averaged in a moving window
124 defined by genomic location. Gene expression in the control cells was weighted according to the
125 probability of gene detection, enhancing the comparison with single cell data, where signal
126 dropout was common for many genes. In a parallel method, the expression disparity values were
127 exchanged for binary values, which were summed cumulatively as a function of genomic
128 location; the gradient of this function yielded a second estimate of CNV that was sensitive to
129 small concordant expression variations in contiguous genes and that was insensitive to large
130 single-gene variations. The CNV estimates of the two methods were combined by their
131 geometric mean.
132
133 **Figure 2** shows sciCNV applied to scRNA-seq data from primary MM cells. Significantly, the
134 CNV profile of a single cell, inferred from its RNA, closely resembles the average CNV profile
135 of $>10^4$ tumor bulk cells, derived from whole exome DNA sequencing (WES) (R^2=0.72) (**figure**
136 **2a-b**). The CNV predictions produced from a single cell by sciCNV were also validated at key

137 locations by FISH (**figure 2c**). Furthermore, examination of >1700 plasma cells from the same
138 MM patient biopsy using sciCNV revealed that the tumor-specific CNV were robustly detected
139 in all of the MMPC (**figure 2d**), despite biological and technical variations between the cells;
140 and were not detected in normal plasma cells (NPC). Thus, sciCNV can utilize scRNA-seq to
141 reveal CNVs in single cells. Moreover, it can distinguish cancer cells and normal cells on the
142 basis of their CNV profile (**figures 2e-f**).
143
144 **Identification of subclones and intra-clonal evolution using scRNA-seq**
145 The detection of CNV with single cells from scRNA-seq data enables the identification of
146 subclones and examination of intra-clonal evolution. Using scRNA-seq, RTAM2 and sciCNV
147 we readily detected up to 7 subclones in primary MM samples comprising <4000 cells (**figure**
148 **3a-b**) and identified an average of 2-3 subclones per sample. Examination of the sciCNV profiles
149 of the individual MM cells yielded evidence of both branching and linear intra-clonal evolution
150 (**figure 3c-d**). In some tumors, marked divergence of two subclones from an inferred ancestral
151 cell was evident, as in **figure 3a, c**; however, in the majority of MM samples examined the
152 subclones diverged at only one or two loci.
153
154 **Dissecting the effects of CNVs on gene expression: +8q23-24 in MM**
155 Simultaneous profiling of both DNA copy number and RNA in the same cell should enable
156 examination of the influence of CNVs on transcriptional programs. To explore this, we used
157 sciCNV to screen MM patient bone marrow samples for tumor cells with +8q24. We sought to
158 examine +8q24 as this is one of the most recurrent abnormalities in human cancer[1,17] and is
159 known to target MYC[18], providing a benchmark for our analyses.
160
161 Using sciCNV, primary MM samples MM199 and MM244 were both found to contain subclonal
162 gains of chromosome 8 encompassing 8q23-24 (**figure 3e**). Both samples also contained closely-
163 related isogenic subclones without +8q. To facilitate gene set enrichment analyses (GSEA)[19] of
164 the intra-tumor subclone pairs, these subclones were next subsampled to yield cellular
165 subpopulations with matching transcriptome depth (**figure 3f**). This prevented subclone biases in
166 total cellular gene expression from influencing specific gene-set detection. The gene expression
167 of the intra-clonal subpopulations, representing isogenic cells with and without +8q23-24, with

168 matched transcriptome sizes, were then compared by GSEA using RTAM2-normalized data.
169 From an analysis of 215 gene sets defined by chromosome location, +8q cells in both samples
170 were strongly enriched for the gene-sets located at 8q23-24, with striking statistical confidence
171 (p=0.000, q=0.000, FWER=0.000), compared to cells without +8q (**supplemental figure S22**).
172 In contrast, no other genomic regions were significantly enriched. Thus, sciCNV accurately
173 resolved single MM cells into intra-tumor subclones, isolating +8q23-24 as a unique variation
174 distinguishing these.
175
176 We next used GSEA to explore the influence of +8q23-24 on cellular programming. As
177 expected, +8q cells from both MM199 and MM244 samples showed increased MYC expression
178 ($p<0.05$) compared to sibling cells without +8q (**figure 3g**). Surprisingly, however, only +8q
179 cells from MM199 showed a broad increase in MYC target genes (p=0.000, q=0.000,
180 FWER=0.000). Canonical MYC signature genes were not upregulated in MM244 +8q cells
181 (p=0.767, FWER=1.0)(**figure 3h**). Nevertheless, from an analysis of 3303 curated gene sets, +8q
182 cells from both MM199 and MM244 tumors showed similar upregulation of gene-sets encoding
183 the machinery of mRNA translation and protein synthesis, including specifically genes involved
184 in 3'UTR-mediated mRNA translation regulation (enrichment rank 5/3303 in MM199 and
185 9/3303 in MM244), ribosome biogenesis (enrichment rank 4/3303 in both) and peptide chain
186 elongation (enrichment rank 3/3303 and 6/3303)(**figure 3h, supplemental figure S22**),
187 potentially representing a more restricted MYC response. Conspicuously, these transcriptional
188 effects of +8q23-24 in MM cells were remarkably close to those of +8q23-24 in breast cancer
189 (FWER p=0.000, enrichment rank 1-2/3303 in both tumors), and this similarity was strong even
190 when MYC hallmark genes were not increased (**figure 3h, supplemental figure S22**). Thus,
191 +8q23-24 induces analogous gene expression changes across malignancies; and these analogous
192 effects are not dependent on broadly-defined MYC-target genes but instead map to the specific
193 upregulation of mRNA translation and protein synthesis.
194
195 The cellular re-programming induced by +8q23-24 might be expected to promote significant
196 increases in gene expression and in cell mass. Notably, however, in the MM samples examined
197 the mTOR-interacting gene, DEPTOR, located at 8q24, was also upregulated in +8q cells (**figure**
198 **3g**), and likely serves to counter increases in cell size, as previously reported[20]. Indeed, from our

199 examination of +8q at a single cell level we uniquely observed that the transcriptome sizes of
200 +8q cells were in fact mildly reduced, compared to sibling cells without the CNV
201 ($p<0.001$)(**figure 3i**). Thus, from a single-cell analysis of +8q23-24 it appears that this CNV acts
202 to boost protein synthesis capacity (ribosomes, translation) without increasing cellular
203 transcriptome size. Ultimately this may lead to enhanced expression of MYC-target genes as
204 proteins in some cancers, but may also serve more broadly to improve the dynamics of protein
205 synthesis and reduce the lag-time required to respond to gene expression changes, potentially
206 enhancing cellular adaptability.
207
208 **The effects of +1q on MM cells**
209 Like +8q23-24, gain of chromosome 1q is highly recurrent in human cancer and is present in
210 >30% of clinical tumors[1,17] Although rare in MM precursor disease, the prevalence of +1q
211 increases significantly in symptomatic MM, more so than any other copy number gain.[18,21] In
212 newly diagnosed MM, +1q is found in 35% of cases and is associated with poor prognosis.[22-29]
213 Despite this, the effects of +1q on cancer cell biology remain poorly understood.
214
215 To examine the cellular effects of +1q, we screened MM patient bone marrows (n=30) by
216 scRNA-seq and RTAM2/sciCNV, and identified ten tumors with +1q (**figure 4a**), including
217 three (MM241, MM244 and MM379) containing synchronous subclones with and without the
218 CNV (**figure 4b**). Although these tumor samples contained 2-6 subclones by sciCNV profiling,
219 the subclones were only partially segregated by expression-based clustering (**supplementary**
220 **figure S23**).
221
222 By GSEA, +1q cells in MM241 showed significant enrichment for all 10 chromosome position
223 gene-sets located at 1q21-1q44 (p=0.000, FDR q<0.005, FWER p=0.000-0.058), while MM244
224 and MM379 +1q cells were correspondingly enriched for gene-sets located at 1q23-1q32
225 (p=0.000, q≤0.004, FWER≤0.019) or 1q22-1q42 (p≤0.004, q≤0.03, FWER≤0.024; 1q23
226 FWER=0.359)(**Figure 5a-b** and **supplementary figures S24-26**). No other genomic regions
227 were significantly enriched, confirming that the intra-clonal +1q subpopulations identified by
228 sciCNV were uniquely divergent at this locus alone.
229

230 We next examined the influence of +1q on transcriptional programs in MM241, MM244 and
231 MM379. Remarkably, the +1q cells in all three tumors showed significant reductions in the
232 unfolded protein response (UPR) compared to their sibling cells lacking +1q ($p<0.003$,
233 FDR≤0.015, FWER≤0.028), suggesting that +1q acts consistently in MM to reduce endoplasmic
234 reticulum (ER) stress (**figure 5b** and **supplementary figures 27-29**). This effect of +1q on the
235 UPR has not previously been reported, though is likely highly advantageous to MM cells, which
236 are professional secretor cells burdened by high proteotoxic stress. In MM241, with the largest
237 +1q CNV, UPR genes EIF4EBP1, EIF4A2, DDIT4, ATF4, ERN1, XBP1 and CEBPB were
238 amongst the genes most downregulated in +1q cells (**figure 5c**). In contrast, ATF6, UAP1 and
239 PSMD4 were incongruously upregulated, likely as result of their location within the 1q gain.
240 With respect to mechanism, we observed that the 1q24 gene EEF1AKNMT, which selectively
241 enhances protein translation in a codon-specific manner[30] to support oncogenic growth[31], was
242 increased in all three +1q subclones, as was TIPRL, which regulates the mTORC1 pathway by
243 inhibiting PP2A and sustaining phosphorylation of EIF4EBP1 and RPS6KB1. In contrast,
244 EIF4A1 or EIF4A2, which jointly promote EIF4E-dependent translation (ET), were reduced, as
245 was the ET-repressor EIF4EBP1 (**figure 5d**). Thus +1q induces complex alterations of
246 translation and of the mTORC pathway that likely influence misfolded protein load. Expression
247 of UAP1 and/or COPA from 1q23 may further alleviate ER stress[32,33].
248
249 Additional +1q effects were observed. Mitochondrial oxidative phosphorylation (OxPhos) and
250 reactive-oxygen gene sets were enriched in MM241 +1q cells, likely driven by the increased
251 expression of COX20, NDUFS2, SDHC, MRPS14 and MRPS21 from 1q21-44 (**figure 5b-c**).
252 However, similar metabolic signatures were not observed in MM244 or MM379, perhaps
253 because MRPS21 (1q21.2) falls outside of the +1q CNV in these later samples, or because
254 enhanced NF-κB signaling may also be required for OxPhos augmentation[34] and was observed
255 only in the MM241 subclone (**supplementary figure S27**), associated with TNFRSF13B over-
256 expression (**figure 5c**).
257
258 Both MM244 and MM379 also showed significant enrichment of E2F, G2M and mitosis
259 programs in +1q cells ($p=0.000$, FDR=0.000, FWER≤0.001) (**figure 5b**) and small increases in
260 cycling cells in G2/M (**figure 5e**), consistent with increased proliferation. However, no increase

261 in proliferation was observed in MM241 +1q cells, indicating that 1q-induced proliferation
262 requires a permissive cellular context. Although CKS1B has been proposed to be mechanistic in
263 +1q-induced proliferation[22,35], we observed no increase in CKS1B in two of the three +1q
264 subclones examined (**figure 5f**), indicating that alternative mechanisms likely drive cell cycling.
265 Overexpression of EEF1AKNMT[31], increased oxidative phosphorylation and reductions in the
266 UPR, may instead contribute to the enhanced proliferation of +1q cells.
267
268 MCL1, a critical anti-apoptosis gene for MMPC[36,37] located at 1q21.2, was also increased 1.45-
269 fold ($p<10^{-9}$) in +1q cells from MM241 (**figure 5f**) in direct proportion to 1q copy number.
270 MCL1 was not however upregulated in either MM244 or MM379, whose 1q gains narrowly
271 excluded the MCL1 locus. Increased MCL1 and apoptotic threshold thus represents an additional
272 function of +1q that may further increase cancer cell aggressiveness.
273
274 A summary of these cellular effects of +1q21-44 in MM is shown in **figure 6a**.
275
276 **Comparison of intra-tumor and inter-tumor CNV studies**
277 We next compared our intra-tumor studies (**figure 6b)** with a traditional inter-tumor study
278 designed to identify the biological role of +1q (**figure 6c**). To perform the inter-tumor study, we
279 examined microarray data from a large published series of MM tumor samples (n=532)
280 characterized by +1q FISH[22] (**supplementary Figures S30-32**). As expected, the MM samples
281 with 1q21 gain by FISH showed enrichment by GSEA for chromosomal position gene sets
282 located at 1q21-44. However, the same samples also showed enrichment for gene-sets located on
283 chromosome 1p22, 13q22, 11q13, 11q22, 5q14, 8q24 and Xq28, compared to tumors without
284 +1q, undermining the value of this cohort for isolating gene expression changes attributable to
285 +1q (**figure 6c**). The samples defined by +1q FISH were also biased towards distinctive MM
286 subtypes, as the +1q cohort included more tumors with t(4;14) while the control samples
287 included more tumors with t(11;14) or hyperdiploidy. Consequently, the utility of these cohorts
288 for the isolation effects specifically attributable to +1q was undermined. GSEA of the cohorts
289 yielded an overabundance of putative +1q-associations whose attribution to +1q or to
290 confounding CNVs or biases in MM subtype was unclear (**figure 6c**).
291

292 Conspicuously, both intra- and inter-tumor studies identified the UPR as a significant +1q co-
293 variant in MM. Strikingly, however, the direction of association differed between the studies,
294 suggesting an error in one of the approaches. Notably, whereas dual profiling of DNA and RNA
295 in single cells enables direct matching of a CNV with its effects on gene expression (**figure 6d**),
296 inter-tumor studies must instead infer associations between CNVs and gene expression from
297 their correlation across unrelated tumors, which can lead to erroneous conclusions as
298 demonstrated in **figure 6e**. Thus, single cell studies of intra-tumor heterogeneity can better
299 isolate CNV-specific effects than traditional multi-tumor bulk profiling studies and may reveal
300 the cellular effects of CNVs with greater accuracy.
301
302 **DISCUSSION**
303 CNVs are critical drivers of cancer biology yet their specific effects on cellular processes remain
304 poorly understood. Here, we report the dual profiling of DNA copy number and RNA within the
305 same cells, using scRNA-seq, and leverage this to explore the effect of CNVs on gene
306 expression. To capture intra-tumor heterogeneity, we profile the RNA and CNVs or thousands of
307 cells per sample. Using these new techniques, we examine the transcriptional effects of copy
308 number gains of chromosome regions 8q23-24 and 1q21-44, representing two of the most
309 common CNVs in human cancer. We show that these lesions induce critical reprogramming of
310 cancer cells that can explain their influence on clinical disease.
311
312 Chromosome +1q is the most common adverse CNV in MM. We demonstrate that +1q causes
313 multiple effects on MM cells including a reduction in the unfolded protein response, which likely
314 results from 1q-associated reconfiguration of translation and from changes in the mTOR
315 pathway. In addition, we demonstrate that primary MM cells with +1q show enhanced oncogenic
316 growth, oxidative phosphorylation and MCL1 expression. Significantly, these specific
317 reprogramming effects may explain the inferior disease control achieved by MM patients with
318 tumors harboring this abnormality, following standard of care therapies[22,26-28,35,38,39]. Thus, the
319 suppression of unfolded protein stress in +1q MM cells may counteract the activity of
320 proteasome inhibitors[26-28], which induce cytotoxicity via ER stress[40,41]. Similarly, the
321 upregulation of MCL1 in cells with +1q21 may counteract treatment-induced apoptosis. And

322 cellular proliferation, which may be induced by 1q-mediated upregulation of EEF1AKNMT, or
323 by UPR reduction, may further contribute to early disease recurrence.
324
325 We demonstrate that the transcriptional effects of +8q23-24 are remarkably similar in MM and
326 breast cancer (FWER p=0.000), irrespective of whether or not hallmark MYC target genes are
327 increased (**figure 3h**). Although +8q23-24 can upregulate the expression of a broad spectrum of
328 MYC target genes, we demonstrate that the transcriptomes of MM cells with +8q are in fact
329 smaller than those of cells lacking +8q, at least in the samples examined by us. Significantly, we
330 demonstrate that a consistent function of +8q23-24 is the upregulation of gene sets involved in
331 mRNA translation, ribosomal biogenesis and peptide elongation. Thus +8q23-24 selectively
332 enhances protein synthesis capacity, without increasing transcriptome size. We propose that this
333 may improve the dynamics of proteome reconfiguration following gene expression changes; and
334 that this may enhance the malleability of cancer cells to environmental challenges.
335
336 We show here that the study of CNVs via single-cell transcriptomics offers a number of
337 advantages. As intra-clonal cells that diverge at a single CNV are virtually isogenic, any
338 consistent divergence in their gene expression can be precisely matched to the subclonal CNV.
339 Furthermore, as the test and control cells are present within the same sample, differences in gene
340 expression due to the microenvironment, clinical factors or due to sample processing are
341 minimized. Inter-tumor cohort studies instead rely upon the identification of correlations
342 between CNVs and gene expression across unrelated samples, and suffer from the substantial
343 additional genetic and clinical heterogeneity that exists between samples. As a result of these
344 limitations, the effects of most cancer CNVs on gene expression remain poorly understood.
345 Fortunately, the compelling benefits of intra-clonal studies suggest that a new era of cancer
346 genomics is emerging in which the precise effects of all cancer CNVs on cellular programming
347 can be determined at the single-cell level. This important knowledge is critical for understanding
348 cancer and for advancing therapeutic strategies that seek to address the foundations of this
349 disease.

REFERENCES

1 Tate, J. G. *et al.* COSMIC: the Catalogue Of Somatic Mutations In Cancer. *Nucleic Acids Res* **47**, D941-D947, doi:10.1093/nar/gky1015 (2019).

2 Taylor, A. M. *et al.* Genomic and Functional Approaches to Understanding Cancer Aneuploidy. *Cancer Cell* **33**, 676-689 e673, doi:10.1016/j.ccell.2018.03.007 (2018).

3 Dey, S. S., Kester, L., Spanjaard, B., Bienko, M. & van Oudenaarden, A. Integrated genome and transcriptome sequencing of the same cell. *Nat Biotechnol* **33**, 285-289, doi:10.1038/nbt.3129 (2015).

4 Han, K. Y. *et al.* SIDR: simultaneous isolation and parallel sequencing of genomic DNA and total RNA from single cells. *Genome Res* **28**, 75-87, doi:10.1101/gr.223263.117 (2018).

5 Macaulay, I. C. *et al.* G&T-seq: parallel sequencing of single-cell genomes and transcriptomes. *Nat Methods* **12**, 519-522, doi:10.1038/nmeth.3370 (2015).

6 Campbell, K. R. *et al.* clonealign: statistical integration of independent single-cell RNA and DNA sequencing data from human cancers. *Genome Biol* **20**, 54, doi:10.1186/s13059-019-1645-z (2019).

7 Fan, J. *et al.* Linking transcriptional and genetic tumor heterogeneity through allele analysis of single-cell RNA-seq data. *Genome Res* **28**, 1217-1227, doi:10.1101/gr.228080.117 (2018).

8 Patel, A. P. *et al.* Single-cell RNA-seq highlights intratumoral heterogeneity in primary glioblastoma. *Science* **344**, 1396-1401, doi:10.1126/science.1254257 (2014).

9 Tirosh, I. *et al.* Dissecting the multicellular ecosystem of metastatic melanoma by single-cell RNA-seq. *Science* **352**, 189-196, doi:10.1126/science.aad0501 (2016).

10 Vallejos, C. A., Risso, D., Scialdone, A., Dudoit, S. & Marioni, J. C. Normalizing single-cell RNA sequencing data: challenges and opportunities. *Nat Methods* **14**, 565-571, doi:10.1038/nmeth.4292 (2017).

11 Lun, A. T., Bach, K. & Marioni, J. C. Pooling across cells to normalize single-cell RNA sequencing data with many zero counts. *Genome Biol* **17**, 75, doi:10.1186/s13059-016-0947-7 (2016).

12 Cole, M. B. *et al.* Performance Assessment and Selection of Normalization Procedures for Single-Cell RNA-Seq. *bioRxiv*, doi:doi: https://doi.org/10.1101/235382 (2017).

13 Stegle, O., Teichmann, S. A. & Marioni, J. C. Computational and analytical challenges in single-cell transcriptomics. *Nat Rev Genet* **16**, 133-145, doi:10.1038/nrg3833 (2015).

14 Vieth, B., Parekh, S., Ziegenhain, C., Enard, W. & Hellmann, I. A Systematic Evaluation of Single Cell RNA-Seq Analysis Pipelines: Library preparation and normalisation methods have the biggest impact on the performance of scRNA-seq studies. *bioRxiv*, 583013, doi:10.1101/583013 (2019).

15 Li, B., Ruotti, V., Stewart, R. M., Thomson, J. A. & Dewey, C. N. RNA-Seq gene expression estimation with read mapping uncertainty. *Bioinformatics* **26**, 493-500, doi:10.1093/bioinformatics/btp692 (2010).

389 16 Hafemeister, C. & Satija, R. Normalization and variance stabilization of single-cell RNA-
390 seq data using regularized negative binomial regression. *Genome Biol* **20**, 296,
391 doi:10.1186/s13059-019-1874-1 (2019).
392 17 Davoli, T., Uno, H., Wooten, E. C. & Elledge, S. J. Tumor aneuploidy correlates with
393 markers of immune evasion and with reduced response to immunotherapy. *Science* **355**,
394 doi:10.1126/science.aaf8399 (2017).
395 18 Misund, K. *et al.* MYC dysregulation in the progression of multiple myeloma. *Leukemia*,
396 doi:10.1038/s41375-019-0543-4 (2019).
397 19 Mootha, V. K. *et al.* PGC-1alpha-responsive genes involved in oxidative phosphorylation
398 are coordinately downregulated in human diabetes. *Nat Genet* **34**, 267-273,
399 doi:10.1038/ng1180 (2003).
400 20 Peterson, T. R. *et al.* DEPTOR is an mTOR inhibitor frequently overexpressed in multiple
401 myeloma cells and required for their survival. *Cell* **137**, 873-886,
402 doi:10.1016/j.cell.2009.03.046 (2009).
403 21 Mikulasova, A. *et al.* Genomewide profiling of copy-number alteration in monoclonal
404 gammopathy of undetermined significance. *Eur J Haematol* **97**, 568-575,
405 doi:10.1111/ejh.12774 (2016).
406 22 Shaughnessy, J. D., Jr. *et al.* A validated gene expression model of high-risk multiple
407 myeloma is defined by deregulated expression of genes mapping to chromosome 1.
408 *Blood* **109**, 2276-2284, doi:10.1182/blood-2006-07-038430 (2007).
409 23 Avet-Loiseau, H. *et al.* Long-term analysis of the IFM 99 trials for myeloma: cytogenetic
410 abnormalities [t(4;14), del(17p), 1q gains] play a major role in defining long-term
411 survival. *J Clin Oncol* **30**, 1949-1952, doi:10.1200/JCO.2011.36.5726 (2012).
412 24 Neben, K. *et al.* Progression in smoldering myeloma is independently determined by the
413 chromosomal abnormalities del(17p), t(4;14), gain 1q, hyperdiploidy, and tumor load. *J*
414 *Clin Oncol* **31**, 4325-4332, doi:10.1200/JCO.2012.48.4923 (2013).
415 25 Walker, B. A. *et al.* A compendium of myeloma-associated chromosomal copy number
416 abnormalities and their prognostic value. *Blood* **116**, e56-65, doi:10.1182/blood-2010-
417 04-279596 (2010).
418 26 An, G. *et al.* Chromosome 1q21 gains confer inferior outcomes in multiple myeloma
419 treated with bortezomib but copy number variation and percentage of plasma cells
420 involved have no additional prognostic value. *Haematologica* **99**, 353-359,
421 doi:10.3324/haematol.2013.088211 (2014).
422 27 Yu, W. *et al.* The amplification of 1q21 is an adverse prognostic factor in patients with
423 multiple myeloma in a Chinese population. *Onco Targets Ther* **9**, 295-302,
424 doi:10.2147/OTT.S95381 (2016).
425 28 Mai, E. K. *et al.* Phase III trial of bortezomib, cyclophosphamide and dexamethasone
426 (VCD) versus bortezomib, doxorubicin and dexamethasone (PAd) in newly diagnosed
427 myeloma. *Leukemia* **29**, 1721-1729, doi:10.1038/leu.2015.80 (2015).
428 29 Hanamura, I. *et al.* Frequent gain of chromosome band 1q21 in plasma-cell dyscrasias
429 detected by fluorescence in situ hybridization: incidence increases from MGUS to
430 relapsed myeloma and is related to prognosis and disease progression following tandem
431 stem-cell transplantation. *Blood* **108**, 1724-1732, doi:10.1182/blood-2006-03-009910
432 (2006).

433 30 Jakobsson, M. E. *et al.* The dual methyltransferase METTL13 targets N terminus and
434 Lys55 of eEF1A and modulates codon-specific translation rates. *Nat Commun* **9**, 3411,
435 doi:10.1038/s41467-018-05646-y (2018).
436 31 Liu, S. *et al.* METTL13 Methylation of eEF1A Increases Translational Output to Promote
437 Tumorigenesis. *Cell* **176**, 491-504 e421, doi:10.1016/j.cell.2018.11.038 (2019).
438 32 Itkonen, H. M. *et al.* UAP1 is overexpressed in prostate cancer and is protective against
439 inhibitors of N-linked glycosylation. *Oncogene* **34**, 3744-3750, doi:10.1038/onc.2014.307
440 (2015).
441 33 Watkin, L. B. *et al.* COPA mutations impair ER-Golgi transport and cause hereditary
442 autoimmune-mediated lung disease and arthritis. *Nature Genetics* **47**, 654 (2015).
443 34 Mauro, C. *et al.* NF-kappaB controls energy homeostasis and metabolic adaptation by
444 upregulating mitochondrial respiration. *Nat Cell Biol* **13**, 1272-1279,
445 doi:10.1038/ncb2324 (2011).
446 35 Zhan, F. *et al.* CKS1B, overexpressed in aggressive disease, regulates multiple myeloma
447 growth and survival through SKP2- and p27Kip1-dependent and -independent
448 mechanisms. *Blood* **109**, 4995-5001, doi:10.1182/blood-2006-07-038703 (2007).
449 36 Tiedemann, R. E. *et al.* Identification of molecular vulnerabilities in human multiple
450 myeloma cells by RNA interference lethality screening of the druggable genome. *Cancer*
451 *Res* **72**, 757-768, doi:0008-5472.CAN-11-2781 [pii]. (2012).
452 37 Derenne, S. *et al.* Antisense strategy shows that Mcl-1 rather than Bcl-2 or Bcl-x(L) is an
453 essential survival protein of human myeloma cells. *Blood* **100**, 194-199 (2002).
454 38 Soriano, G. P. *et al.* Proteasome inhibitor-adapted myeloma cells are largely
455 independent from proteasome activity and show complex proteomic changes, in
456 particular in redox and energy metabolism. *Leukemia* **30**, 2198-2207,
457 doi:10.1038/leu.2016.102 (2016).
458 39 Morales, A. A. *et al.* Distribution of Bim determines Mcl-1 dependence or codependence
459 with Bcl-xL/Bcl-2 in Mcl-1-expressing myeloma cells. *Blood* **118**, 1329-1339,
460 doi:10.1182/blood-2011-01-327197 (2011).
461 40 Obeng, E. A. *et al.* Proteasome inhibitors induce a terminal unfolded protein response in
462 multiple myeloma cells. *Blood* **107**, 4907-4916, doi:10.1182/blood-2005-08-3531 (2006).
463 41 Bianchi, G. *et al.* The proteasome load versus capacity balance determines apoptotic
464 sensitivity of multiple myeloma cells to proteasome inhibition. *Blood* **113**, 3040-3049,
465 doi:10.1182/blood-2008-08-172734 (2009).
466 42 Ledergor, G. *et al.* Single cell dissection of plasma cell heterogeneity in symptomatic and
467 asymptomatic myeloma. *Nat Med* **24**, 1867-1876, doi:10.1038/s41591-018-0269-2
468 (2018).
469 43 Zhan, F. *et al.* The molecular classification of multiple myeloma. *Blood* **108**, 2020-2028,
470 doi:10.1182/blood-2005-11-013458 (2006).

SUPPLEMENTARY INFORMATION:

Methods and supplementary figures can be found on-line.

ACKNOWLEDGEMENTS:

The authors thank the patients, their families and the physicians who made this study possible. They also thank N. Winegarden, N. Khuu and G. Basi in the Princess Margaret Genomics Facility and Z. Lu in the Princess Margaret Bioinformatics Core for technical assistance; and Drs. Gary Bader and Caleb Stein for independent critical review and comments. This work was supported by funding from The Princess Margaret Cancer Centre Foundation, the Terry Fox Foundation and the Canadian Cancer Society Research Institute.

Author Contribution

A.M-S performed research and analyzed data. N.E., C.L-H. and I.T. performed FISH, FACS and whole exome sequencing, respectively. P.N. provided essential reagents. R.E.T. designed research, analyzed data and wrote the paper.

Competing interests

The authors declare that they have no competing interests.

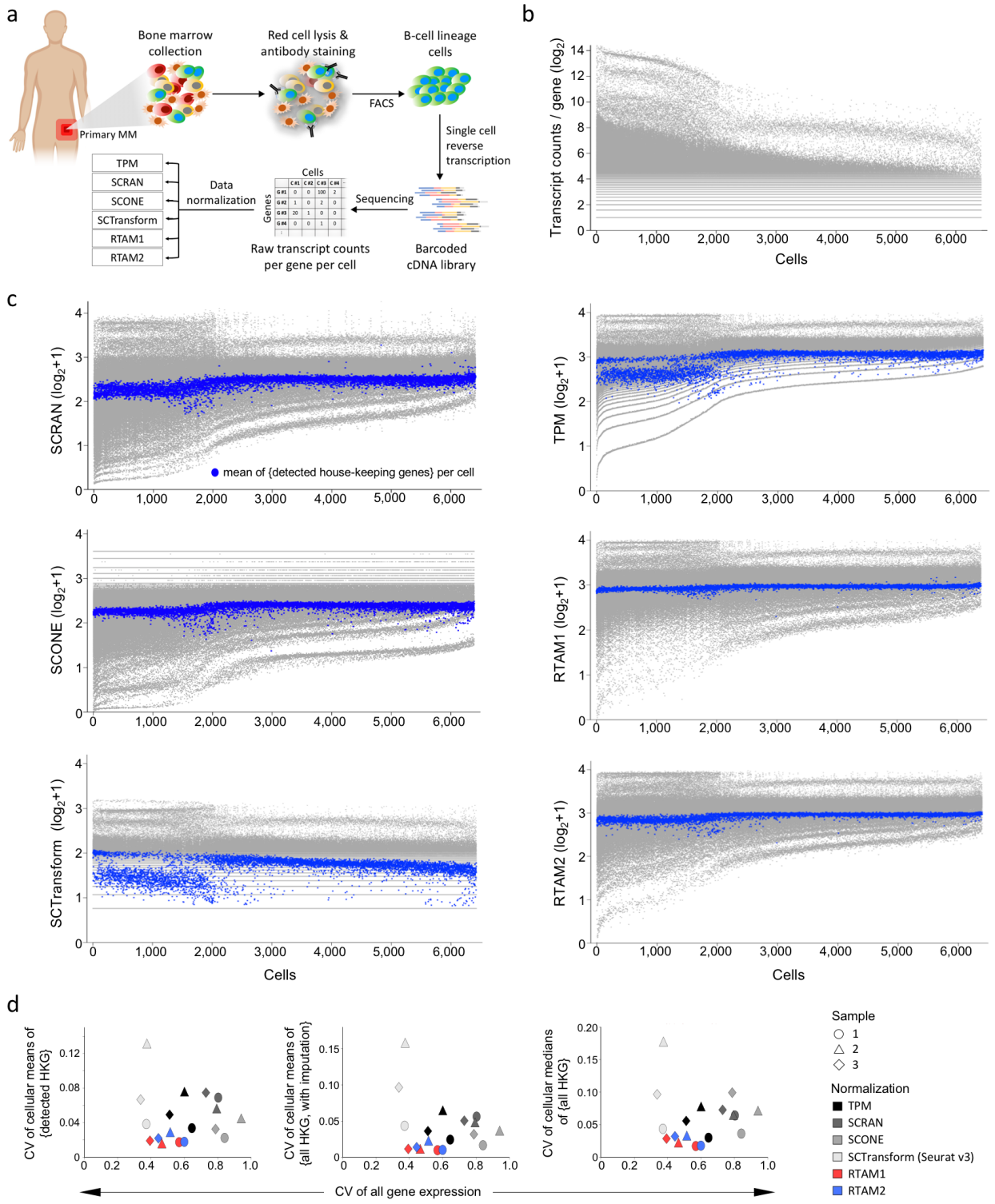

Figure 1. Comparison of scRNA-seq normalization strategies

a. Overview of workflow. MM, multiple myeloma. FACS, fluorescence activated cell sorting. **b.** Plot of scRNA-seq data from >6,000 cells of B cell lineage, isolated from the bone marrow of a

MM patient, depicting the raw (pre-normalized) transcript counts per gene per cell. Each dot represents an integer transcript count for one or more genes in a single cell; cells (columns) are ranked from left to right by their total transcript count. **c.** The same data is shown following normalization using TPM, SCRAN, SCONE, SCTransform, RTAM1 or RTAM2 methods (and following log transformation). To compare the methods, the mean expression (blue) of a curated set of house-keeping genes (HKG) is plotted in each cell, omitting genes with zero values due to non-expression or detection "drop-out". **d.** The coefficient of variation (CV) across cells in the average expression of HKGs within each cell is shown for 3 patient samples containing >15,000 cells. The average HKG expression in each cell was calculated in 3 different ways as either the mean of the detected HKG (left panel), the mean of all HKG [with imputation of null "dropout" values] (middle panel), or the median of all HKG without imputation (right panel). As the various normalization methods expand or compress the distribution of the overall gene expression data to different extents, the CV of HKG averages is plotted against the CV of expression of all genes.

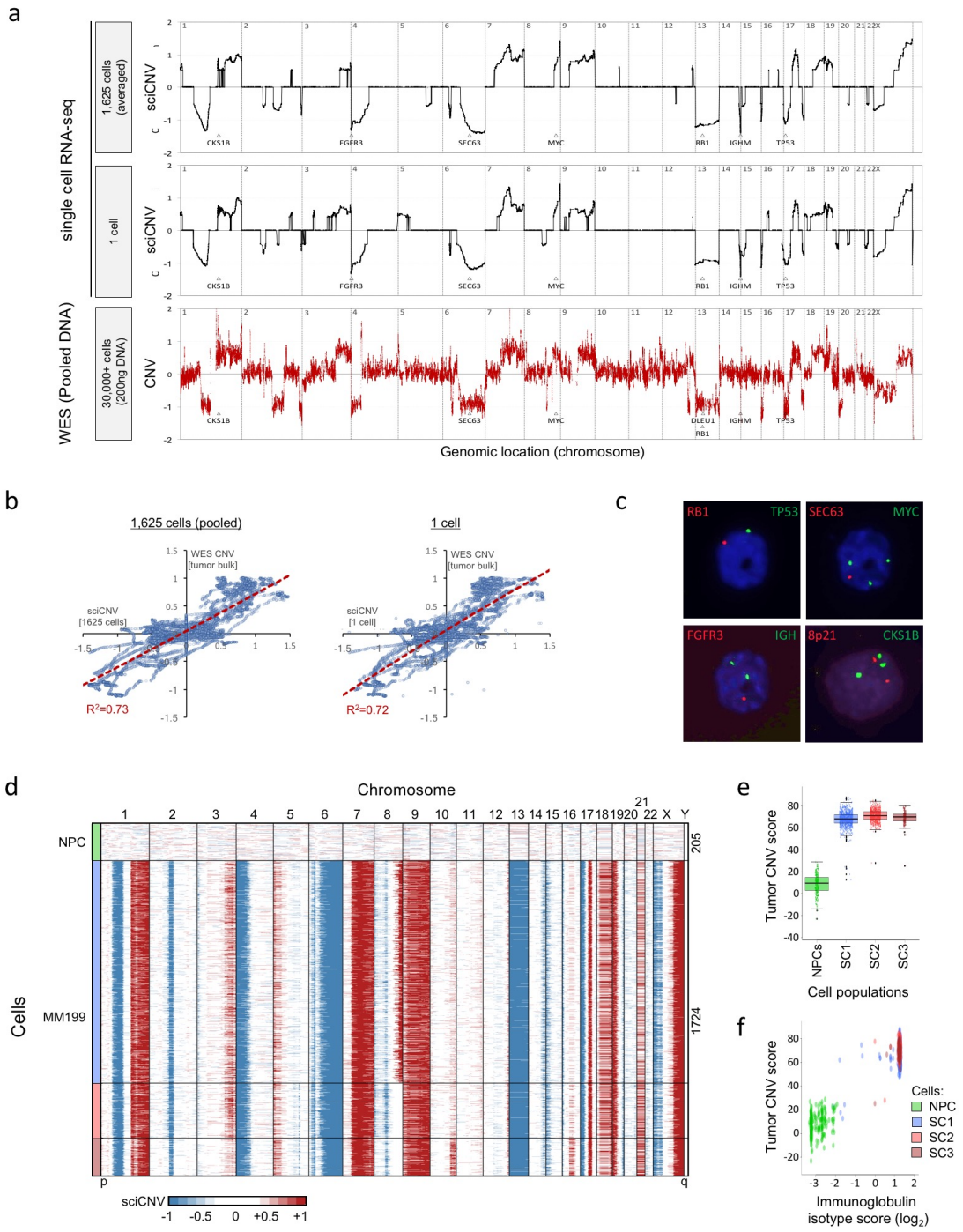

Figure 2. Single cell inferred chromosomal copy number variation (sciCNV)

a. The inferred CNV profiles of 1,625 pooled MM cells (top panel) or of a single MM cell (middle panel) were calculated from scRNA-seq data using RTAM2/sciCNV and are shown compared with the CNV profile of bulk tumor cells (lower panel), which was determined by whole exome sequencing (WES) of 200ng DNA (representing >30,000 complete exomes)

23 purified from $1.9x10^6$ cells. Cells were isolated from bone marrow by FACS. **b.** Correlation of
24 the scRNA-seq sciCNV profiles from (a) with the tumor bulk CNV profile derived from WES.
25 For the correlation, the CNV results from sciCNV and WES were paired by genomic location
26 and averaged over similar chromosomal segment lengths; sciCNV results were generated
27 without a noise cut-off filter. **c.** FISH was also used to verify sciCNV–derived copy number
28 predictions, focusing on the genes highlighted in **a.**; this showed 3 copies of CKS1B (1q21), 1
29 copy of FGFR3 (4p16), 1 copy of SEC63 (6q21), 2 copies of PNOC (8p21), 3 copies of MYC
30 (8q24), 1 copy of RB1 (13q14,) and 1 copy of TP53 (17P13) in accordance with sciCNV
31 predictions derived from the RNA of a single cell. Brightness and contrast were adjusted during
32 figure construction to enhance probe visualization. **d.** Heatmap showing chromosome copy
33 number gains (red) and losses (blue) in individual multiple myeloma plasma cells (MMPC,
34 n=1724), inferred from scRNA-seq using sciCNV. The MMPC are grouped into subclones
35 (coloured bars at left) and their CNVs are compared with that of normal plasma cells (NPC,
36 n=205, green bar) from a control sample. **e.** Identification of malignant cells using scRNA-seq
37 and sciCNV. The tumor plasma cells in subclones (SC) 1-3 in **d.** were distinguishable from NPC
38 on the basis of the similarity of their individual sciCNV profiles to the mean tumor clone
39 sciCNV profile, calculated as a 'tumor CNV score'. **f.** Validation of cancer cell identification by
40 the tumor CNV score. The tumor CNV scores for single cells are shown plotted again a cellular
41 immunoglobulin-isotype score, derived to distinguish cells expressing immunoglobulin of the
42 tumor clone isotype from polyclonal cells expressing other isotypes. Virtually all cells with a
43 high tumor CNV score also expressed immunoglobulin of the tumor isotype. Whereas
44 immunoglobulin restriction is only informative for lymphoid malignancies the tumor CNV score
45 can be applied to all tumor types.

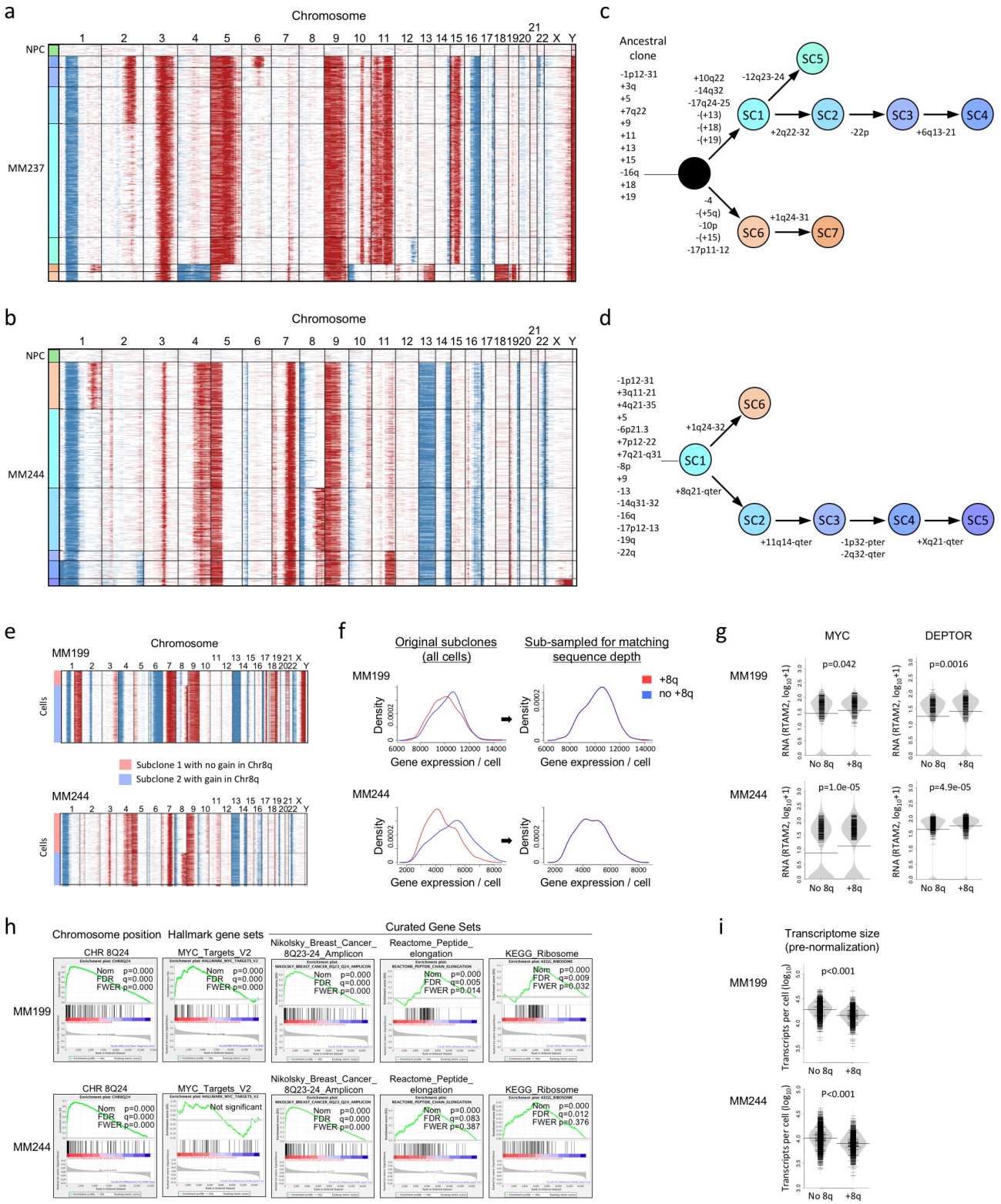

46 **Figure 3. Examination of subclones with 8q gain at single cell resolution using sciCNV.**

47 **a.** and **b.** The sciCNV profiles of plasma cells from multiple myeloma patient bone marrow

48 samples MM237 (**a**) and MM244 (**b**) were calculated using scRNA-seq and are shown compared

to normal plasma cells (NPC). The tumor cells in each sample are grouped into subclones (colour bars at left) distinguished by divergent CNV. **c.** and **d.** Possible evolutionary paths for the subclones detected in MM237 and MM244, revealing branching and linear intra-clonal evolution. Subclones (SC) are represented by coloured circles corresponding to the colour bars in **a.** and **b.**

e. Heatmaps showing the sciCNV profiles of near isogenic subclone cells in MM199 and MM244 that that diverge at +8q. **f.** The distribution of total gene expression per cell (normalized transcriptome size) for the subclones shown in **e**. The subclones were sampled for subpopulations of cells with matching transcriptome sizes (right panel), which were then compared in subsequent panels (**g.-i.**). **g.** Bean plots showing the mRNA expression (RTAM2) of MYC or DEPTOR genes, located on chromosome 8q24, in transcriptome size-matched subpopulations from MM199 or MM244, by +8q status. Expression is plotted on $\log_{10}$ scale. P-values were calculated by t-test. **h.** Results of gene set enrichment analysis (GSEA) performed on subpopulations of MM199 and MM244 cells, comparing cells with or without +8q. The analysis of chromosome position gene sets (n=215) shows highly-significant enrichment of gene sets located on chromosome 8q23-24 in the populations of cells identified at single cell resolution as containing +8q by sciCNV (left panels). Key results of GSEA for hallmark (n=49) and curated (n=3303) gene sets are shown in the middle and right panels, demonstrating broad upregulation of MYC target genes in MM199 +8q cells, but not in MM244 +8q cells, and upregulation of ribosome and peptide_elongation signatures in +8q cells from both tumors; the expression changes attributable to +8q in MM cells from both tumors strongly resemble those found in breast cancer cells with an 8q23-24 amplicon. **i.** Bean plots showing the pre-normalized transcriptome sizes of subclonal MM cells from MM199 or MM244, demonstrating slightly fewer RNA transcripts in cells with +8q. P-values were calculated by t-test.

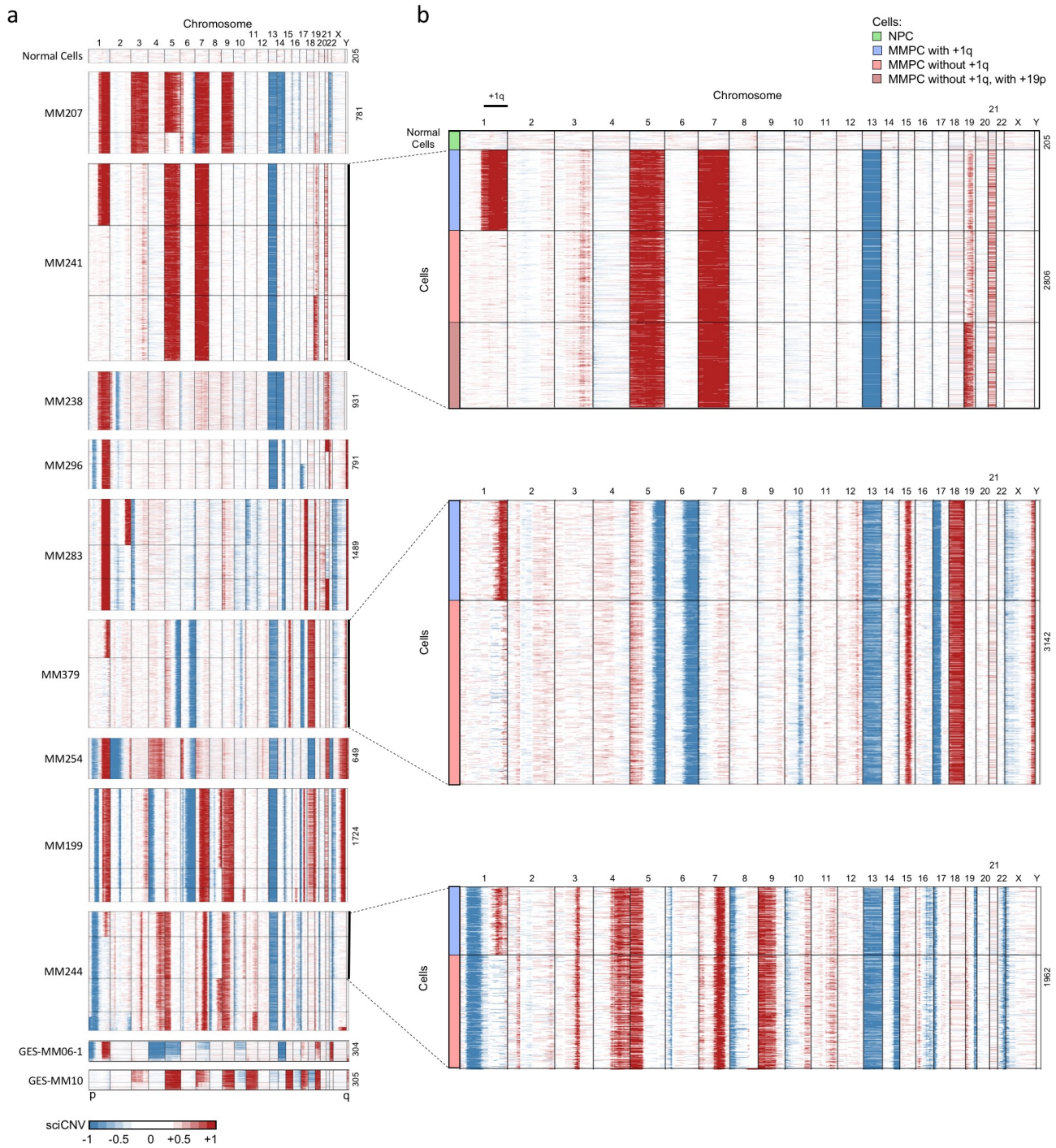

Figure 4. sciCNV profiles of MM samples with chromosome 1q gain.

a. The CNV profiles of MM cells (n=16,299) from 10 MM tumor samples with chromosome 1q gain, inferred from scRNA-seq by sciCNV. The profiles of normal plasma cells (n=205) are shown at the top. The number of cells in each sample is shown at the right. Samples containing >3,000 cells are scaled by 0.5x for figure construction. Samples GES-MM06-1 and GES-MM10

78 at the bottom were characterized by MARS-seq[42]; single cell CNV predictions are shown here
79 calculated on the MARS-seq data using sciCNV.
80 **b.** Magnified view of MM241, MM379 and MM244, which were identified by sciCNV as
81 containing sibling subclones with and without gain of chromosome 1q (blue and red bars at left).

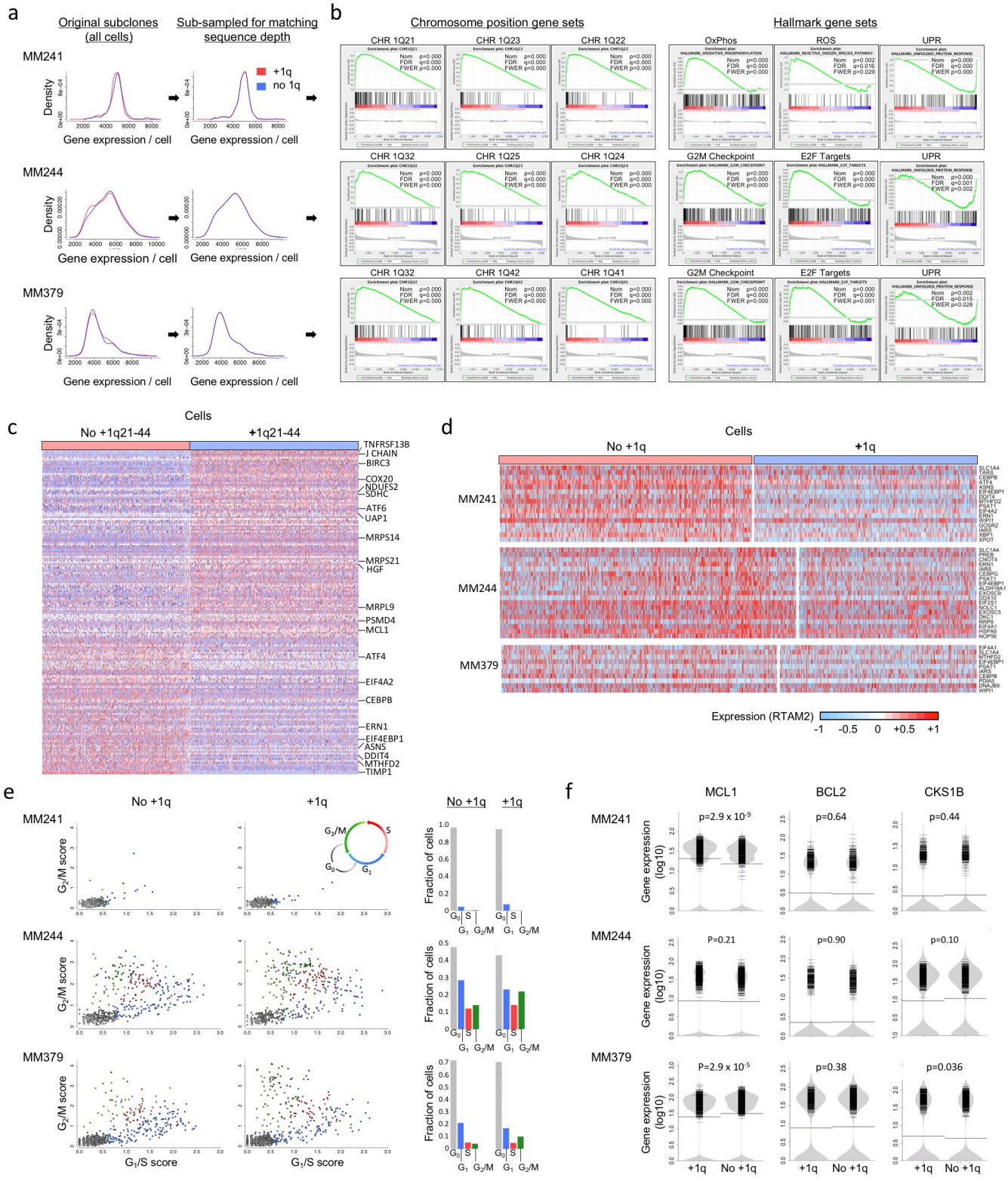

Figure 5. The effects of +1q on cellular programs in primary MM cells

a. The total gene expression (mRNA per cell) of cells in MM241, MM244 and MM379 with or without +1q (left column), demonstrating that +1q has no effect on transcriptome size (unlike

85 +8q). The subclones were nevertheless subsampled for subpopulations that were matched for
86 transcriptome depth (right column), which were examined in the subsequent studies. **b.** Results
87 of GSEA comparing sciCNV-resolved primary MM cells with or without +1q using RTAM2-
88 normalized transcriptomics data. Analysis of chromosome position gene sets (n=215) revealed
89 highly-significant enrichment for 1q gene sets in the cells identified individually as containing
90 +1q by sciCNV (left panels). GSEA results for hallmark gene sets are shown at the right. G2M,
91 E2F, oxidative phosphorylation (OxPhos) and reactive oxygen species (ROS) gene sets were
92 variably enriched in subclones with +1q, while the UPR was decreased in all subclones with +1q.
93 **c.** Heatmap depicting the differential gene expression of MM cells with or without +1q from
94 sample MM241 (which contains a full-length +1q21-44 CNV). Columns represent cells and rows
95 represent genes. **d.** Heatmaps showing the differential expression of UPR genes in cells with or
96 without +1q, for MM241, MM244 and MM379 patient samples. **e.** Cell cycle phase of matched
97 primary MM cells from the 3 patient samples, comparing cells with or without +1q. Cells were
98 assigned to a cell cycle phase (colour-coded as per the legend) and plotted according to their
99 relative expression of gene sets associated with G1/S and G2/M. The fraction of cells in each
100 phase according to +1q status is summarized by histogram (right). **f.** Bean plots depicting the
101 relative expression of MCL1 (located at 1q21.2) and CKS1B (1q21.3) in cells with or without
102 +1q. The expression of BCL2 (located at 18q21) is shown as a control. Expression is plotted on a
103 $\log_{10}$ scale. P-values were calculated by t-test.

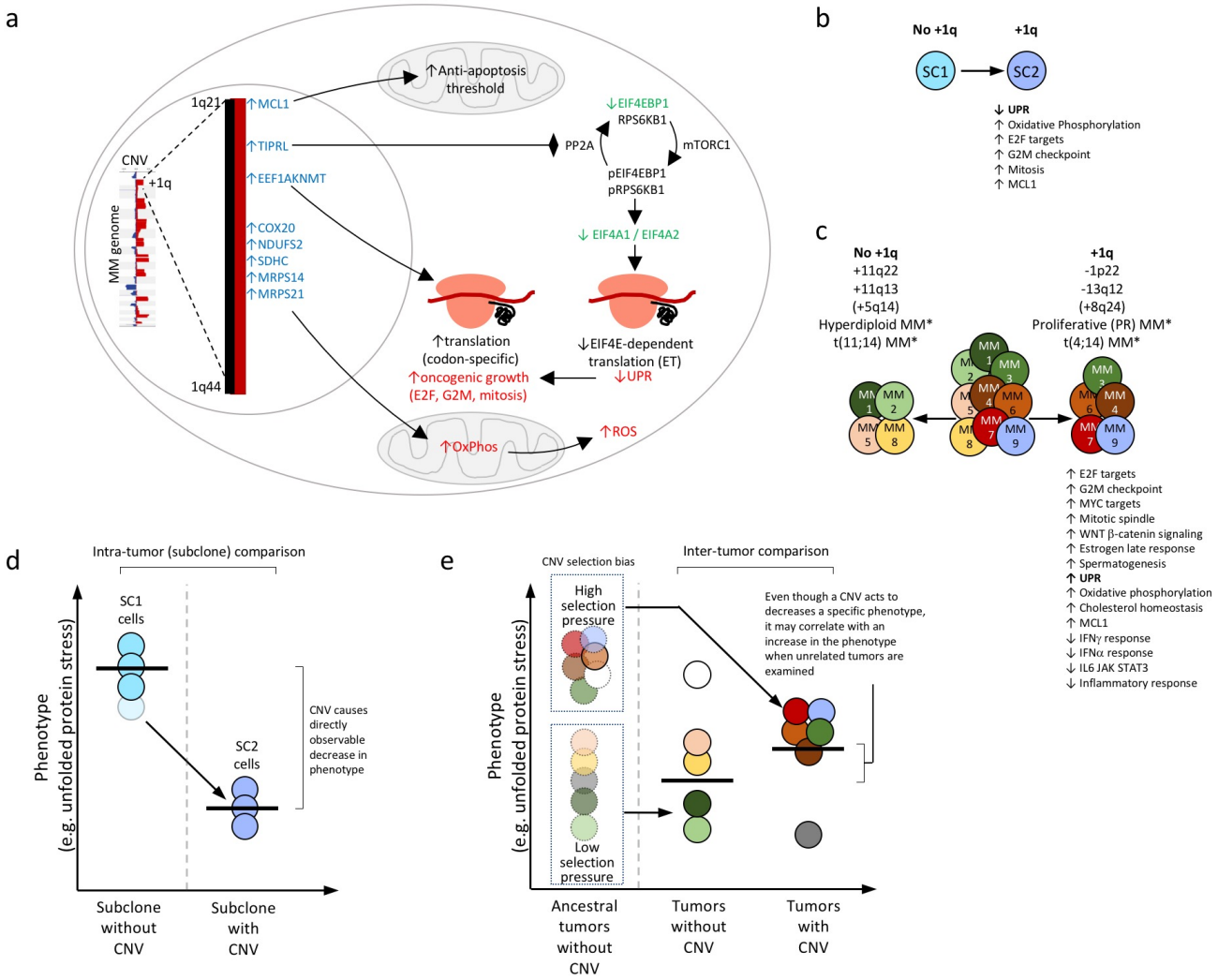

Figure 6. The effect of +1q on cellular programs in MM and comparison of intra-tumor and inter-tumor studies.

a. Summary of the influences of +1q21-44 on MM cell biology, as determined by scRNA-seq. Genes located on 1q that are increased in +1q cells (blue) are linked to downstream subcellular programs that altered by +1q (red) via intermediate genes that also show altered expression in +1q cells (green).

b. and **c.** Comparison of intra-tumor and inter-tumor studies to determine the effects of +1q in MM. **b.** The results of intra-tumor GSEA of MM241, MM244 and MM379 are summarized. Amongst chromosome position gene sets, only 1q gene sets were enriched in +1q cells. The hallmark gene sets that were significantly co-modulated are shown. **c**. The results of an inter-tumor analysis addressing the same biological question are summarized. MM tumor cohorts from GSE2658[22] (n=532 samples) were defined by the presence or absence of +1q by FISH.

116 Chromosome position gene-sets that were significantly divergent between the cohorts by GSEA
117 are listed above the graphic. Gene sets with nominal p-value<0.05 but FWER p-value>0.05 are
118 bracketed. Although large numbers of tumor samples were grouped specifically according to
119 their 1q status, additional genomic heterogeneity persists between the cohorts. Biases in MM
120 genetic subtypes(*), correlating with +1q status, were also observed, as reported[22,43]. Hallmark
121 gene sets that were divergent between the cohorts are listed below the schema. MCL1 expression
122 was analyzed at single gene level.
123 **d.** Illustration of an intra-tumor analysis of sibling subclones. The effect of a divergent CNV on
124 transcriptional programs can be directly assessed. The subclones are otherwise isogenic,
125 reducing the influence of confounding genetic variations, and are derived from the same sample,
126 minimizing the influence of confounding variations due to sample processing, batch effect or
127 recent patient treatment.
128 **e.** Illustration of an inter-tumor analysis in which the influence of a CNV on cell phenotype is
129 examined, highlighting potential biases. In the example, the CNV does not occur randomly but is
130 preferentially selected for by tumors experiencing a specific stressor (left column). The gene
131 expression of the tumor cohorts that do or do not develop the CNV are therefore not identical at
132 baseline. Although the CNV may act to reduce the stressor, it's occurrence may appear to
133 correlate with increased rather than with decreased stress, or may fail to correlate.